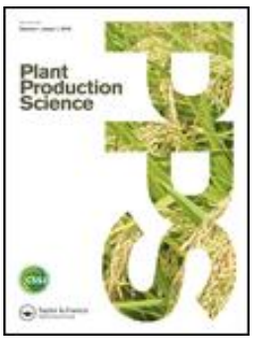

Plant Production Science

ISSN: 1343-943X (Print) 1349-1008 (Online) Journal homepage: http://www.tandfonline.com/loi/tpps20

Development and verification of a simulation model for paddy drying with different flatbed dryers

Nguyen Van Hung, Romualdo Martinez, Tran Van Tuan & Martin Gummert

To cite this article: Nguyen Van Hung, Romualdo Martinez, Tran Van Tuan & Martin Gummert (2018): Development and verification of a simulation model for paddy drying with different flatbed dryers, Plant Production Science, DOI: 10.1080/1343943X.2018.1518723

To link to this article: https://doi.org/10.1080/1343943X.2018.1518723

Accepted author version posted online: 05 Sep 2018.
Published online: 01 Oct 2018.

PLANT PRODUCTION SCIENCE
https://doi.org/10.1080/1343943X.2018.1518723

Development and verification of a simulation model for paddy drying with different flatbed dryers

Nguyen Van Hung[a], Romualdo Martinez[b], Tran Van Tuan[c] and Martin Gummert[a]

[a]Sustainable Impact Platform, International Rice Research Institute (IRRI), Los Baños, Luzon, Philippines; [b]Bioprocess Engineering Division, Philippine Center for Postharvest Development and Mechanization, Munoz, Nueva Ecija, Philippines; [c]Center for Agricultural Energy and Machinery, Nong Lam University, Ho Chi Minh City, Vietnam

ABSTRACT

This research developed a computer-based simulation model applicable for conventional and reversible airflow flatbed dryers, which can be used to predict the optimized time for mixing paddy (for the conventional flatbed dryer) and reversing the drying air (for the reversible air flatbed dryer). The developed software has the ability of simulating the paddy moisture content and temperature based on the input parameters of ambient (temperature and relative humidity) and drying air (temperature and airflow rate), dimensions of the dryers, and input grain properties and weight. The model was verified based on data collected from actual paddy drying practices in Vietnam from 1994 to 2015. Relative errors between modeled and measured moisture content of paddy varied for different stages of the drying process and different dryer capacities. On average, the error was highest at the middle stage of the drying processes. This error increased gradually during the early two-thirds stage of the drying process and reached 19% and 14% for the conventional and reversible air flatbed dryers, respectively. On the other hand, these errors decreased to less than 10% at the end of the drying process. Accurate prediction of optimized machine operating time determines the uniformity of the final moisture content of paddy between top and bottom layers, improving energy efficiency, and reducing postharvest losses and drying cost.

ARTICLE HISTORY
Received 15 June 2018
Revised 11 August 2018
Accepted 28 August 2018

KEYWORDS
Rice; postharvest; drying; flatbed dryer; modeling; simulation

1. Introduction

About 500 million tonnes of milled rice are produced in the world annually (Ricestat, 2017). Postharvest processes, including the operations from harvesting to milling cause losses both in quantity and quality in the range of 20–30% of rice grain produced (FAO, 2013). Drying is a postharvest process in which the moisture content is reduced to a safe level for storage. Drying is considered to be the most important process of all postharvest activities (RKB, 2017). Delayed drying, incomplete drying, or inefficient drying leads to reduction in rice quality and increase in postharvest losses (RKB, 2017; Xiao & Gao, 2008).

Drying technologies and many types of mechanical dryers were developed for paddy drying from farm scales to industrial scales, and are covered in many publications, such as Brooker et al., (1974) and RKB (2017). Among those dryer types, the flatbed dryer (FBD) is one of the most common types for cereal dryers in Asia (Lopez et al., 1998; Zare et al., 2009). This dryer type is widely used for paddy drying in Southeast Asian countries as they are fixed with the desired scales, have relatively low investment and cost, and low management capacity requirement (Phan et al., 1995; Gummert, 2013). Design layouts, performance, and adaptation of FBDs to different conditions are presented in many publications, such as RKB (2017), Gummert (2013), Phan et al. (1995), and Tado et al. (2015). The grain bulk is contained in a rectangular bed, on an elevated perforated floor, which is on top of a plenum chamber. Drying air is heated by being mixed with flue gas from a furnace, which usually uses rice husk as it is one of the lowest-cost fuels for paddy drying (Nguyen et al., 2017; Nguyen et al., 2018). The heated drying air is then forced by the blower through the grain bulk to generate a heat and mass transfer process consisting of the evaporation and removal of water from paddy grains. The drying process is continued until the average grain mass is dried to the desired MC for storage and milling, usually 14% (RKB, 2017).

Drying is a process of heat and mass transfers (Chua, et al., 2002). Its performance to minimize grain quality loss needs to be optimized for maximum energy efficiency; and its cost is affected by many factors, such as structure of the

CONTACT Nguyen Van Hung hung.nguyen@irri.org

dryers, environment, temperature and relative humidity of ambient and drying air, static pressure of drying air, grain temperature, initial moisture content of grain, etc. Developing simulation models for the drying process is very important to understand how the related factors influence drying, for optimizing dryer performance without having to run many costly and time consuming drying trials.

Deep-bed drying models are usually developed based on thin-layer models. There were many thin-layer models developed for paddy drying, such as in the works of Wongwises and Thongprasert (2000), ASAE (1999), Chen (1998), Abe and Afzal (1997), Chen and Shei (1996), Jindal and Siebenmorgen (1994), and Islam and Jindal (1981). More recently, based on the thin-layer models above, various computer-based simulation models for deep-bed drying were also presented in related researches by Nguyen et al., (2016), Tajaddodi (2012), Zare and Chen (2009), Zare et al., (2006), Felipe and Barrozo (2003), Martinez (2001), and Sitompul et al., (2001).

However, there is no publication on a simulation model that covers both options of the conventional flatbed dryers (FBDc) and the reversible air flow flatbed dryers (FBDr). To initiate the development of such a drying model, this research developed a computer-based combined simulation model that can be used for FBDc and FBDr. The model was then verified with data measured from actual practices of drying long-grain paddy in Vietnam.

2. Methodology

2.1. Assessments of flat bed dryers

The modeling and verification were developed for optimizing the management of the different types of FBDs that were recently adopted in Southeast Asia and are described in Phan et al. (1995), Gummert (2013), and Tado et al. (2015). These FBDs (Figure 1(a)) consist of three main components: (1) a furnace to generate heat, (2) a blower to generate drying air with the required airflow rate and static pressure, and (3) a drying chamber. A FBD with the drying air moving in one direction (by default upwards) is called FBDc, whereas when its drying air can move in two directions either upward or downward as shown in Figure 1(b), it is called FBDr. The drying material is loaded into the drying bin on top of a perforated floor with a depth of 25–40 cm or 50–60 cm for the FBDc or FBDr, respectively; and the drying air temperatures are in the ranges of 42–45°C for grain and 40–43°C for seed production (Gummert, 2013; Phan et al., 2003).

2.2. Mathematical modeling of the deep-bed drying process

The general approach to mathematically describing the drying process in a grain bed is to divide the process into small sub-processes. The drying process is considered to occur in thin layers over a series of discrete time intervals. Starting from the first layer at the air inlet portion, the drying air passes through each layer as shown in Figure 2. Heat and moisture balance equations describe the condition of the air and the grain layer after each time interval, with the exhaust air condition from one layer used as the inlet air condition to the next layer. The layer-by-layer calculations are done through the entire bed over a series of time interval until drying is completed. For reversed airflow, the same layer by layer calculations are followed, except that the drying air enters the bed in the opposite downward direction, starting from the last (top most) layer and exiting from the first (bottom most) layer.

The near-equilibrium model developed by Thompson et al., (1968) and Thompson (1972) was adopted in this study. Figure 3 shows the basic input and output parameters of the model. The inlet air with temperature, T_o, humidity ratio, H_o, and superficial air velocity, v, passes through the thin layer for a drying time interval, Δt. The thin layer has a current moisture content, M_o, and grain temperature, θ_o. Moisture is evaporated into the drying air resulting in a reduction in moisture content, M_f, and increase in humidity ratio, H_f, of the exhaust air. The temperature of the exhaust air, T_f, is reduced in proportion to the increase in grain temperature, θ_f, through the evaporative cooling that occurs during moisture evaporation. The amount of moisture removed per unit of time is determined by the thin-layer drying equation. The final heat balance equation determines the final air and grain temperatures.

Thompson et al. (1968) model was applied to determine the equilibrium drying air temperature and equilibrium moisture content based on the following procedure:

- First, a sensible heat balance is performed to determine the equilibrium drying air temperature (T_e). All the heat and mass balances are presented in kg^{-1} dry air basis.

$$c_a T_0 + H_0(h_{v0} + c_v T_0) + C_g \theta_0 = c_a T_e + H_0(h_{v0} + c_v T_e) + C_g \theta_e \quad (1)$$

$$C_g = c_g R \quad (2)$$

$$R = \frac{\rho_g \Delta x (1 - M_{owb}/100)}{60\, v\, \Delta t\, \rho_a} \quad (3)$$

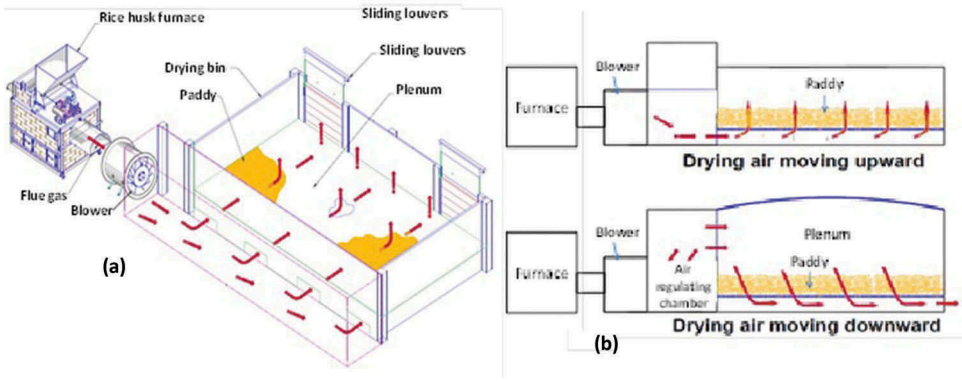

Figure 1. Flatbed dryer (FBD) showing the schematic diagram (a) and principle schema of drying airflow directions moving up- and down-ward (b).

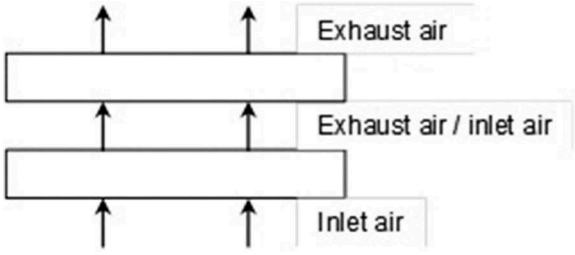

Figure 2. Simulation of grain drying in a deep bed as series of thin-layer drying processes.

where

T_o = inlet air temperature, °C
T_e = equilibrium drying air temperature, °C
θ_o = initial grain temperature, °C
θ_e = equilibrium grain temperature, °C, equal to T_e
H_o = inlet air humidity ratio, kg kg^{-1}
c_a = specific heat of dry air, 1.005 kJ kg^{-1} °C^{-1}
c_v = specific heat of water vapor, 1.850 kJ kg^{-1} °C^{-1}
h_{vo} = latent heat of vaporization of free water at reference, 2500.8 kJ kg^{-1}
C_g = specific heat of grain, converted to kJ kg^{-1} air °C^{-1}
c_g = specific heat of grain, kJ kg^{-1} °C^{-1} (see Table 1)
R = dry matter to dry air ratio for each layer and time interval, kg kg^{-1}
M_{owb} = initial moisture content of the grain bed, % wet basis (w.b.)
ρ_g = bulk density of grain, kg m^{-3} (see Table 1)
ρ_a = density of air, kg m^{-3} (ASAE, 1997)
Δx = depth of thin layer, m
Δt = time interval, min
v = superficial air velocity, m s^{-1}

- Next, the equilibrium moisture content, M_e, of the thin-layer is determined by first calculating the relative humidity, RH_e, which corresponds to T_e and, H_o and then using the RH_e and T_e values in the equilibrium moisture content equation,

$$M_e = \frac{1}{100}\left[\frac{\ln(1 - RH_e/100)}{-0.000035502\,(T_e + 27.396)}\right]^{1/2.31} \quad (4)$$

where

M_e = equilibrium moisture content, % dry basic (d.b.)
RH_e = equilibrium relative humidity, %

The T_e in all thin-layer changes as drying progresses. A new drying curve is specified when the T_e changes and the amount of drying in the previous curve has to be transformed to the current curve. This transformation

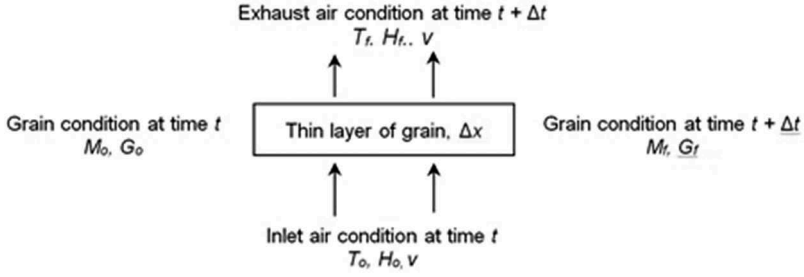

Figure 3. Input and output parameters of the near-equilibrium model.

Table 1. Grain properties used in the deep-bed simulation model.

Property	Equation	
Thin-layer drying and rewetting (Martinez, 2001)	$MR = \frac{M_f - M_e}{M'_o - M_e} = \exp(-kt^n)$	(13)
	For drying	
	$k = \exp(-13.882 + 2.3712 \ln(T_o) - 0.50207 \ln(H_o))$	(14)
	$n = \exp(1.7203 - 0.30364 \ln(T_o) + 0.26821 \ln(H_o))$	(15)
	For rewetting	
	$k = \exp(-4.0935 + 0.86339 \ln(T_o) - 1.2070 \ln(M_o))$	(16)
	$n = \exp(-0.10295 + 0.12368 \ln(H_o) + 0.082250 \ln(M_o))$	(17)
Equilibrium relative humidity (ASAE, 1997)	$RH_e = 100\left[1 - \exp(-0.000035502\,(T_e + 27.396)\,M_e^{2.31})\right]$	(18)
Bulk density (Wratten et al., 1969)	$\rho_g = 519.4 + 5.29 M_{owb}$	(19)
Specific heat (Wratten et al., 1969)	$c_g = 0.921 + 0.0545\, M_{owb}$	(20)
Latent heat of vaporization (Hunter, 1989)	$\Delta L = R_v\,(T_e + 273.16)^2 \left[\frac{1 - RH_e/100}{RH_e/100}\right] 0.000035502\, M_e^{2.31}$	(21)
Resistance to airflow (Martinez, 2001)	$\Delta P' = \frac{6290\, v^2}{\ln(1 + 5.58\, v)}$	(22)

R_v = gas constant for water vapor, 461.5 J kg^{-1} °C^{-1}; $\Delta P'$= specific resistance to airflow, Pa m^{-1}.

was made by calculating the equivalent drying time, t_e. Based from the thin-layer drying equation,

$$t_e = \left[-\frac{1}{k} \ln\left(\frac{M'_o - M_e}{M_o - M_e}\right)\right]^{1/n} \tag{5}$$

where

M_o = current moisture content of the thin-layer, % d.b.

M'_o = initial moisture content of the grain bed, % d.b.

MR = moisture ratio, dimensionless

t_e = equivalent drying time, min

k, n = drying/rewetting constants (see Table 1) evaluated at T_e, H_e, M'_o

The t_e is the equivalent drying time needed for the drying curve to reach the current moisture content. The final moisture content, M_f, at the end of the current time interval,Δt, is then calculated from the thin-layer drying equation using the time, $t_e + \Delta t$,

$$MR = \frac{M_f - M_e}{M_o - M_e} = \exp\left[-k\,(t_e + \Delta t)^n\right] \tag{6}$$

where

M_f = final moisture content, % d.b.

The amount of moisture removed from the grain, equal to $M_o - M_f$ percentage points, is evaporated to the air, thereby increasing the humidity ratio by the amount,ΔH,

$$\Delta H = \frac{(M_o - M_f)}{100} R \tag{7}$$

and the final humidity ratio is calculated as,

$$H_f = H_o + \Delta H \tag{8}$$

where

H_f = final humidity ratio, kg kg^{-1}

ΔH = change in humidity ratio, kg kg^{-1}

The final temperature is determined from the final heat balance,

$$\begin{aligned} &c_a T_e + H_0(h_{v0} + c_v T_e) + C_g\theta_e + c_w(H_f - H_0)\theta_e \\ &\quad = c_a T_f + H_f(h_{v0} + c_v T_f) + C_g\theta_f + \Delta L(H_f - H_0) \end{aligned} \tag{9}$$

where

T_f = final air temperature, °C

θ_e = equilibrium grain temperature equal to T_e, °C

θ_f = final grain temperature equal to T_f, °C

c_w = specific heat of water, Eqn. 186 kJ kg^{-1} °C^{-1}

ΔL = difference between latent heat of vaporization of water in grain and free water, kJ kg^{-1}

The Thompson (1972) model, simplification of the Thompson et al. (1968) model, was then applied in the simulation. This later model assumes moisture equilibrium between the air and the thin-layer of grain during each time interval. No thin-layer drying or rewetting equation is required to determine the amount of moisture removed or added. The following balances are solved to determine the equilibrium conditions between the air and a particular grain layer during each time interval. All heat and mass balances are in kg^{-1} dry air basis.

Heat balance between the air and the grain,

$$\begin{aligned} &c_a T_0 + H_0(h_{v0} + c_v T_0) + C_g\theta_0 + c_w(H_f - H_0)\theta_0 \\ &\quad = c_a T_f + H_f(h_{v0} + c_v T_f) + C_g\theta_f \end{aligned} \tag{10}$$

Mass balance between the air and the grain,

$$H_f - H_o = \frac{(M_o - M_f)}{100} R \tag{11}$$

Equivalence between the relative humidity of the air and equilibrium relative humidity of the grain as described by ERH equation,

$$ERH_f = 100\left[1 - \exp(-0.000035502\,(T_f + 27.396)\,M_f^{2.31})\right] \tag{12}$$

The air relative humidity, RH, which corresponds to the given air temperature, T, and humidity ratio, H, is calculated from the properties of moist air from ASAE (1997).

The grain properties used in the mathematical models are summarized in Table 1. The moist air properties were adopted from ASAE (1997).

Within this study, the model was applied for FBD with drying temperature lower than 45°C. However, this model can also be used for higher drying temperature situations:

- The original Thompson et al. (1968) model was used for simulating high temperature corn drying
- The thin-layer drying equation of Martinez (2001) used in this study can be used for low and high temperature drying. It was based on laboratory experiments with the range of drying temperature between 30 and 90°C.

2.3. Methodology of verifying the model

The developed model was verified through comparative assessments of the drying processes from the modeled results with measured data. Measurements were conducted *in-situ* by sampling paddy during actual drying practices in Vietnam. Figure 4 shows the schematic top-view of a FBD with six sampling positions (1, 2, 3, 4, 5, and 6). At each position, paddy samples were collected at the two layers, top and bottom. For the small FBDs with their capacity lower than 1.5 t batch^{-1} with a small drying bin, the samples were just collected at 4 points of 1, 2, 5, and 6 as shown in Figure 4.

Table 2 shows the data collected from the simulations and from experiments of actual dryers for paddy drying using different sizes of FBDc and FBDr. These data were synthesized into the average values of:

- Dimension of drying chambers shown in their *Length*Width (m*m)*
- Ambient air properties: temperature (°C) and relative humidity (RH %)
- Drying air properties: temperature (°C), velocity measured at the surface of grain bulk (m s^{-1})
- Paddy: Initial weight in a drying batch (kg), Moisture content MC (%) at input and during drying process (the interval was 1–2 h).

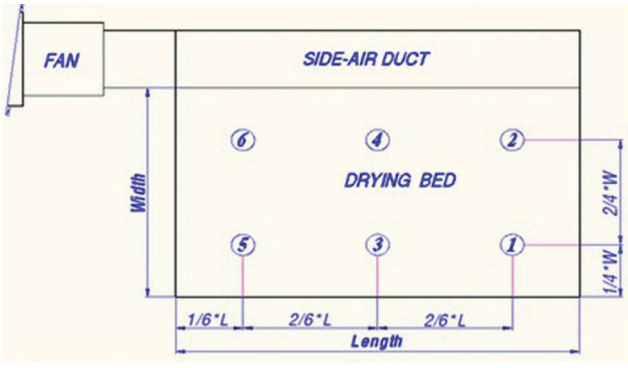

Figure 4. Schematic diagram of sampling positions (top-view of the FBD). *L = Lenght of a dryer's side; W = Width of a dryer's side.*

2.4. Software and data analysis

A simualtion program was created based on the mathematical modeling for FBDc and FBDr. This program, called FBD Drying Simulation Beta (FBD-Simulation), has its interface as shown in Figure 5. We then use FBD-Simulation to estimate the paddy drying process and record the data for MC reduction of the top and bottom layers and drying time to obtain the required MC of grain.

Grain MCs during drying processes simulated from FBD-Simulation were then compared with that measured from actual practices for evaluation and verification. Comparison between the modeled MC ($MC_{modeled}$) and measured MC ($MC_{measured}$) is presented through the index, so called error (*ERR*), calculated based on Equation (23).

$$ERR(\%) = \frac{|\mathrm{MC}_{\mathrm{modeled}} - \mathrm{MC}_{\mathrm{measured}}|}{\mathrm{MC}_{\mathrm{modeled}}} * 100 \qquad (23)$$

Where:

$MC_{modeled}$: estimated (modeled) moisture content of grain resulted from the FBD-Simulation.

$MC_{measured}$: moisture content of grain measured during the experiments or actual practices.

3. Results

3.1. Conventional flatbed dryers (FBDc)

Comparisons of paddy MC between measured and modeled data for the experimental FBDc 0.5 t batch^{-1} (FBDc0.5) and actual operation FBDc6 t batch^{-1} (FBDc6) are shown in Figure 6. As the results, for both practices of FBDc0.5 and FBDc6, reduction rate of grain MC in the early two-thirds (2/3) of drying time was lower from actual measurements, than that generated from modeling. It means that the actual process was slower than the modeled process in the early drying stage. However, the drying time to attain the required final grain MC is not much different between the measured and modeled results. For the FBDc0.5, drying times to reduce grain MC from 20% down to 14% were about 7.5 h and 7.0 h for the actual and modeled scenarios, respectively. For the FBDc6, drying

Table 2. Data of paddy drying assessed with different flatbed dryers.

#	Dryers	Drying chamber	Ambient air		Drying air		Paddy				Source of data
		Length*width (m*m)	°C	RH (%)	°C	Velocity (m s^{-1})	Initial weight (kg)	Thickness of grain layer (cm)	Initial MC_{wb} (%)	Final MC_{wb} (%)	
1	FBDc0.5	2*1	27.9	88	40.7	0.19	549	48	19.9	13.3	Le, 2011
2	FBDc4	5*3	30.0	75	38.7	0.20	3526	41	22.5	14.3	Phan, Nguyen, Nguyen, Le, & Truong, 2000
3	FBDc6	5*4	24.8	85	41.6	0.19	5107	44	26.2	13.0	Le, 2011
6	FBDr0.1	0.3*0.3	27.0	75	43.0	0.20	36	69	25.2	13.3	Lam, 2004
8	FBDr1.5	2*2	31.5	75	43.3	0.21	1620	70	28.5	15.0	Phan et al., 2003
9	FBDr4	4*3	26.4	75	35.5	0.22	3716	53	20.6	14.0	Nguyen, Nguyen, Le, & Phan, 2009
10	FBDr8	7*4	24.9	85	36.7	0.22	7500	46	23.0	13.3	Le, 2011
11	FBDr10	7*5	32.6	75	40.9	0.27	9000	44	25.1	14.1	Tran, Tran, Nguyen, & Nguyen, 2015

FBDc = conventional flatbed dryer; FBDr = reversible air flow flatbed dryer; The number (no.) after FBD(c or r) is its capacity (t batch^{-1}); MC_{wb} = Moisture content in wet basis.

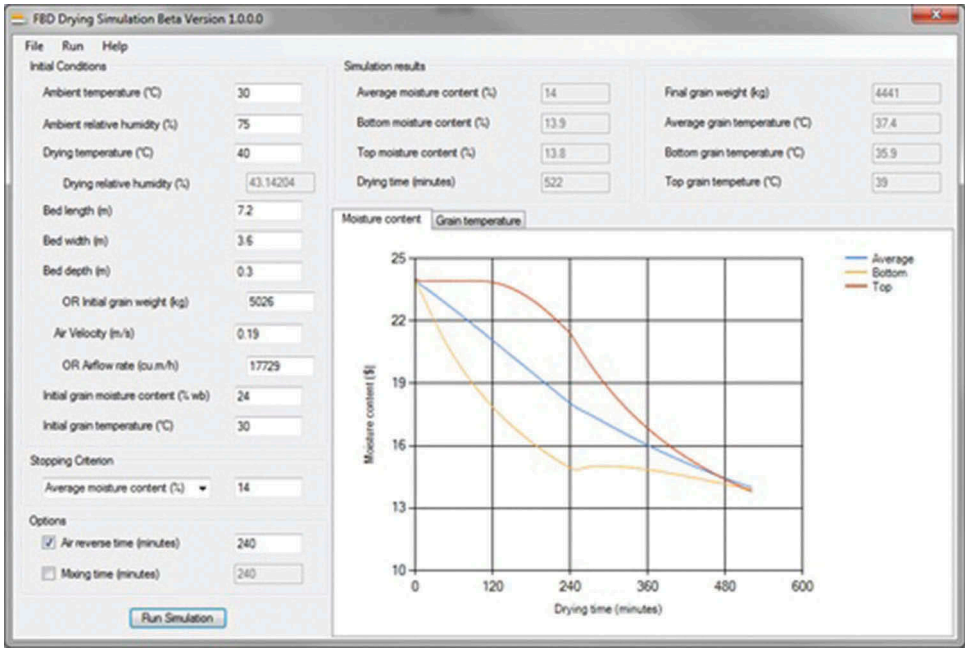

Figure 5. Interface of the beta version for FBD simulation.

time for reducing grain MC from 26% down to 14% was about 9 h for both actual and modeled scenarios.

Comparisons of actual and modeled drying processes for various FBDc with different capacities from 0.5 to 6 t batch^{-1} are shown in Figure 7. Paddy MCs measured during actual drying at both the top layer (Measured-top) and bottom layer (Measured-bottom) fluctuated much more than those resulting from modeling. On average, the MC reduction of Modeled-bottom was faster than that of Measured-bottom during the early stage of drying time (ranging from 0 to 5 h of the drying process). Drying rate (MC reduction by time) of the bottom layer from modeling was about 20–30% higher than that of actual drying. In the middle stage of drying process (Figures 6 and 7), grain moisture content in the model was lower than that of the actual measure because of the following possible reasons:

- The actual MC was the average from measuring in different drying batch and different points in each batch, whereas the modeled MC was just estimated from one input MC.
- In the actual practices, the density of the wet grain bulk may also cause a reduction of the drying rate.

The relative errors (%) between modeled and measured MCs during the drying processes for different FBDc are also shown in Figure 7. The error of the bottom layer reached 19%, while that of the top layer was less than 10%. Highest errors happened in the early stage of

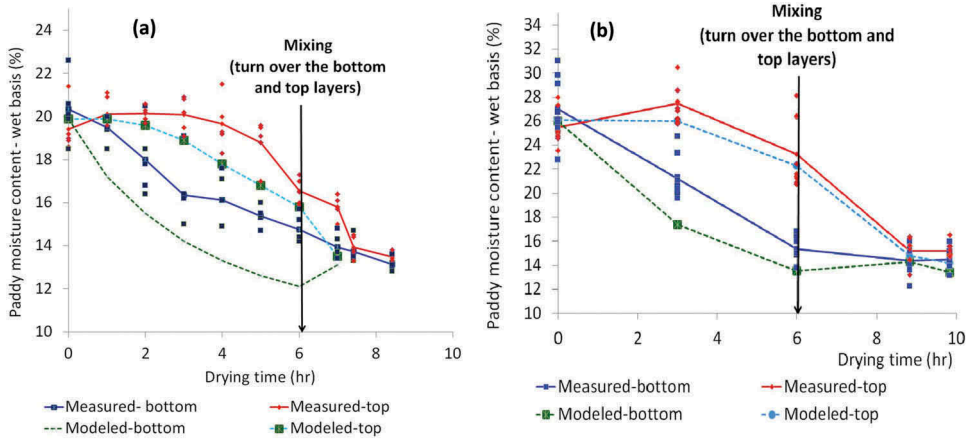

Figure 6. Moisture content reduction in paddy drying with FBDc0.5 (a) and FBDc6 (b). *Markers in the graphs represent for the data measured at different points of the paddy bulk.*

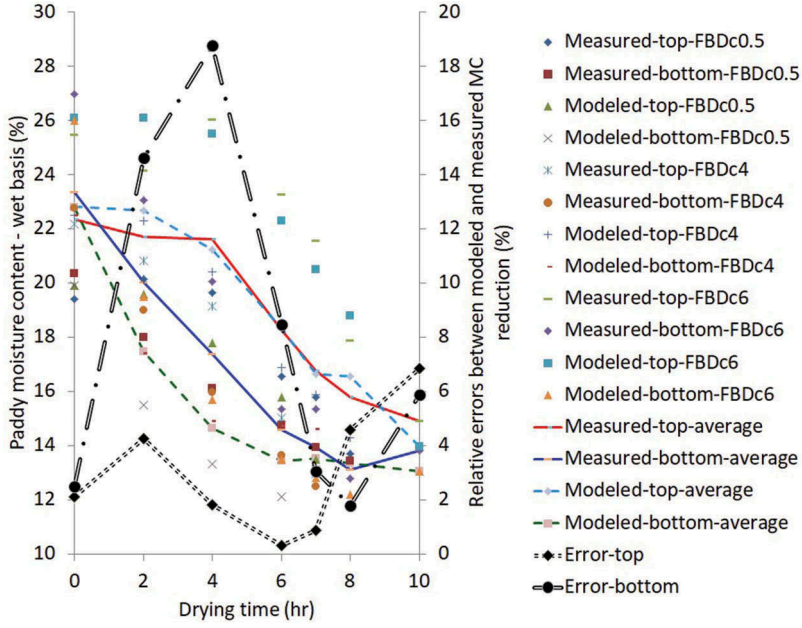

Figure 7. Comparisons of actual and modeled drying processes for different FBDc. *Measured-top and measured-bottom = measured MC at the top and bottom layers of drying paddy; Modeled-top and modeled-bottom: Modeled (estimated) MC at the top and bottom layers of drying paddy; FBDc(x) = Conventional flatbed dryer with (x) t batch^{-1}; Markers in the graph represent for data of the different FBDc from 0.5 to 6 t batch^{-1}.*

drying, at the time interval from 2 to 5 h. However, after about two-thirds of the drying time (after mixing the paddy), the errors of both bottom and top layers are almost the same; decreasing to less than 10% when the drying process is finished. Possible causes of the error are described in the discussion section.

3.2. Reversible air flow flatbed dryers (FBDr)

Similarly, comparisons between measured and modeled paddy MC for the experimental FBDr with 0.1 t batch^{-1} (FBDr0.1), and the actual operation FBDr with 10 t batch^{-1} (FBDr10) are shown in Figure 8. For FBDr0.1, the difference between the actual and modeled paddy MC of the bottom layer was very low, whereas that of the top layer was much higher. On the other hand, these differences were not significant for FBDr10. The error between the modeled and measured paddy MC for the experimental dryer (FBDr0.1) was higher than that for the actual dryer (FBDr10). This was because the model used was already adapted for actual paddy drying with adjusted coefficients.

In addition to the comparison between actual and modeled drying processes of FBDr, an investigation of

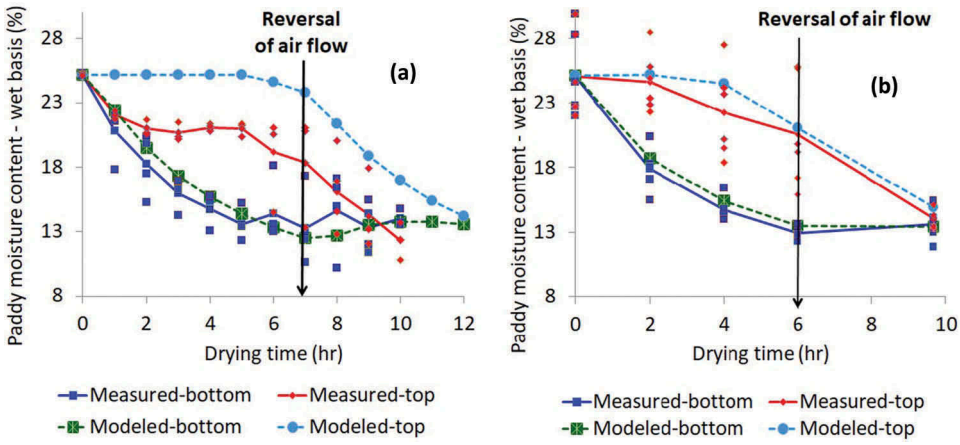

Figure 8. Moisture content reduction of paddy drying with FBDr0.1 (a) and FBDr10 (b). *Markers in the graphs represent for the data measured at different points of the paddy bulk.*

the paddy MC reductions for various FBDr with different capacities resulted in the drying curves shown in Figure 9. Paddy MCs measured during the actual drying at both the top layer (Measured-top), and bottom layer (Measured-bottom) with FBDr fluctuated more compared to those from the modeled paddy MC. On average, the drying time from modeling of drying paddy with MC from 24% down to 14% was 12 h, or 10% longer than that of the actual drying process. This 10% or 1 h over-estimation of time required for drying may affect the operation plan or scheduling of the system. Then again, for batch drying systems, the total operation time usually fluctuated more than 10% depending on many other factors, such as labors, loading and unloading, etc.

To attain the final MC of 14%, the average MC reduction lines of bottom and top layers intersected at earlier points (about 15% MC in this case) and then the gap was re-expanded at the end point of 14% MC. These less optimized processes should be affected by many related drying factors, such as paddy bulk, drying air properties, mixing time, etc.

The relative errors (%) between modeled and measured MCs during drying processes for the researched

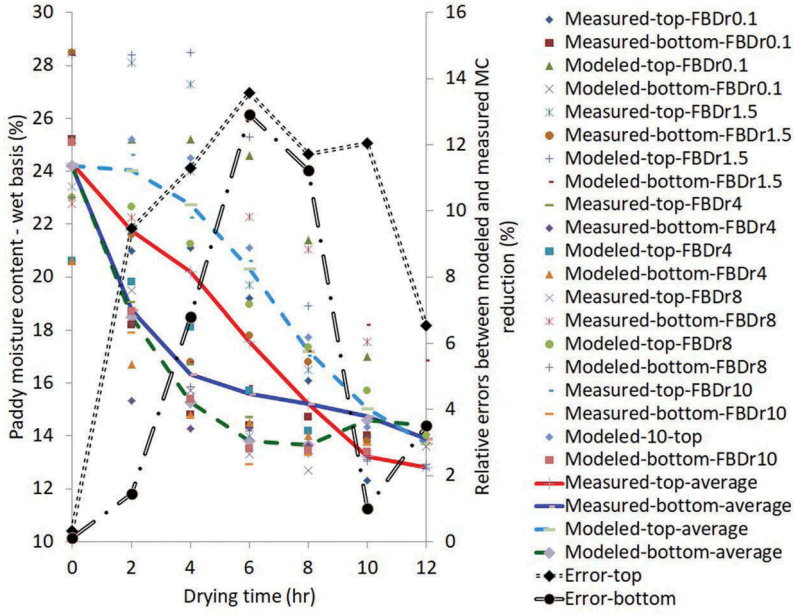

Figure 9. Comparisons of actual and modeled drying process for different FBDr. *Measured-top and measured-bottom = measured MC at the top and bottom layers of drying paddy; Modeled-top and modeled-bottom: Modeled (estimated) MC at the top and bottom layers of drying paddy; FBDr(x) = Conventional flatbed dryer with (x) t batch^{-1}; Markers in the graphs represent for data of the different FBDr from 0.1 to 10 t batch^{-1}.*

Table 3. Timing of mixing grain and reversing airflow.

Dryer	Initial weight (kg)	Initial MC_{wb} (%)	Final MC_{wb} (%)	Drying temperature (°C)	Timing for mixing grain or reversing drying air (h)	Drying time (h)	Percentage of drying process (%)
FBDc0.5	549	19.9	13.3	40.7	6	7.5	80
FBDc4	3526	22.5	14.3	38.7	6	8	75
FBDc6	5107	26.2	13.0	41.6	6	9	67
FBDr0.1	36	25.2	13.3	43.0	7	10	70
FBDr1.5	1620	28.5	15.0	43.3	6	8	75
FBDr4	3716	20.6	14.0	35.5	4	6	67
FBDr8	7500	23.0	13.3	36.7	7.5	12	63
FBDr10	9000	25.1	14.1	40.9	6	9.5	63

FBDc = conventional flatbed dryer; FBDr = reversible air flow flatbed dryer; The number (no.) after FBD(c or r) is its capacity (t batch^{-1}); MC_{wb} = Moisture content in wet basis.

FBDrs also varied much for different FBDrs with different capacities. These errors were in the range of 0–14%. The errors between modeled and measured MCs increased gradually to the highest points of about 10–14% at the middle of drying process and then reduced to less than 10% after that. However, the error of the top layer slightly increased again at the end of the drying process for about 2%. This might be because of improper selection of the air reversing time. This illustrates an advantage of the model to estimate the optimized reversal point of airflow, to reach the optimized drying process and obtain the uniform final moisture content of paddy.

3.3. Timing for mixing grain and reversing drying air

Table 3 shows the timing for mixing grain (for FBDc) and reversing drying air (for FBDr) applied for the research dryers. Time from starting the drying process to mixing grain for FBDc ranged from 67 to 80% of the total drying process, while that to reversing drying air for FBDr ranged from 63 to 75%. Fluctuation of this parameter depends on many factors, such as properties of grain, ambient and drying air, and the capacity of dryers. However, the model established can estimate the optimized value for this parameter.

4. Discussion

This computer-based simulation model was developed using the near-equilibrium models of Thompson et al. (1968) and Thompson (1972). The Thompson (1972) model assumes both thermal and moisture equilibrium between the air and the grain over each layer during each time interval. On the other hand, the Thompson et al. (1968) model also assumes thermal equilibrium, but the moisture transfer rate is governed by the characteristic thin-layer drying or rewetting equation. For this reason, the two models would give different estimates of the final air and grain condition for each layer during each time interval. In this study, these values were compared and the better estimates were chosen for the next calculation steps.

Every drying model is developed for some specific drying condition which is determined by the type of machine, paddy variety, weather condition, drying parameters, etc. Accuracy of the simulation models are affected by not only specific drying materials and conditions but also the thin-layer based models. This accuracy is usually represented by the relative error in percentage between the drying parameters predicted from modeling and measured from experiments. Verification of this simulation model indicated the lower accuracy for the early two-thirds stage of drying process. The relative errors (%) between modeled and measured moisture content of paddy during the early two-thirds stage of drying process reached up to 19% and 14% for FBDc and FBDr, respectively. However, at the end of drying process, these errors decreased to less than 10% for both conventional and reversible air FBDs.

Generally, the relative error of this simulation model is higher than the range of 10–15% error reported in other publications, such as Sitompul et al. (2001), Madhiyanon et al., (2001), Dimitriadis and Akritidis (2004), Kalbasi (2003), and Tang et al., (2004). Verification of the model in this research indicated a higher error than that of the others. This would be mainly caused by that the verification resulted in this research was based on the actual practices whereas that of other researches were conducted through laboratory experiments. For instance, ambient parameters (i.e. temperature and relative humidity) are controlled during the laboratory experiments but not for the actual practices.

This computer-based simulation model can be used to predict the optimized time for mixing paddy (for FBDc) and reversing air (for FBDr). Drying process thus would be improved to obtain the uniformity of final MC

of paddy (i.e. 14%) between top and bottom layers in a minimum drying time. This would result in increasing drying efficiency and reducing drying cost.

The model established could also be applied for FBDs without limitation in capacity. It has high potential for application to higher capacity FBDs (30–50 t batch^{-1}) that are popularly used in Vietnam.

However, there are still large gaps between the modeled and actual results; thus, this model would need improvement to minimize the relative errors with the actual practices. Further research should be conducted to have a simulation comparing the gradient of the final moisture contents of the top and bottom layers for dryers with air reversal, as well as without air reversal. Optimized drying process and airflow reversal based on simulation would result in minimizing the moisture gradient among different layers of paddy in a FBD, and would minimize grain brokenness in the next milling process.

5. Conclusion

This research resulted in a computer-based simulation model and its verification for conventional and reversible air FBDs. The developed software has the ability of simulating the paddy moisture content and temperature over time based on the input parameters of ambient and drying air, dimensions of the dryers, and input grain properties and weight. This study resulted in a tool that would significantly help predict and optimize the paddy drying processes using FBDs.

A verification of this simulation model was conducted based on the comparison of grain MC reduction between predicted data from modeling and measured data from samples taken from actual dryers. As the results, actual measured data fluctuated much more than those gained from modeling. Relative errors between modeled and measured MCs during the drying processes for the researched FBDs varied for the different stages of the drying process, different dryer types (i.e. FBDc and FBDr), and different dryer capacities. Generally, the error was highest at the middle stage of the drying processes. This increased gradually during the early two-thirds stage of the drying process and reached to 19% and 14% for FBDc and FBDr, respectively. On the other hand, these errors typically decreased to less than 10% at the end of the drying process.

One of the biggest potentials of this computer-based simulation model is the prediction of the optimized time for mixing paddy (for FBDc) and reversing air (for FBDr), by evaluating which timing leads to the most uniformly dried paddy at the end of the drying process. The results from the simulation can be used to increase the uniformity of the final MC of paddy between the top and bottom layers, thus improving energy efficiency and reducing postharvest losses and drying cost.

Nomenclature and units

% w.b.	% moisture content in wet basis
% d.b.	% moisture content in dry basis
θ_o	initial grain temperature, °C
θ_e	equilibrium grain temperature, °C
θ_f	final grain temperature equal to T_f, °C
c_a	specific heat of dry air, kJ kg^{-1} °C^{-1}
C_g	specific heat of grain, kJ kg^{-1} air °C^{-1}
c_v	specific heat of water vapor, kJ kg^{-1} °C^{-1}
Eqn	Equation
FBD	Flatbed dryer
FBDc	Conventional flatbed dryer
FBDr	Reversible airflow flatbed dryer
h_{vo}	latent heat of vaporization of free water at reference, kJ kg^{-1}
H_f	final humidity ratio, kg kg^{-1}
H_o	inlet air humidity ratio, kg kg^{-1}
MC	moisture content in wet basis (%)
M_e	equilibrium moisture content, % d.b.
M_f	final moisture content, % d.b.
M_o	current moisture content of the thin-layer, % d.b.
M_{owb}	initial moisture content of the grain bed, %w.b.
MR	moisture ratio, dimensionless
R	dry matter to dry air ratio for each layer and time interval, kg kg^{-1}
R_v	gas constant for water vapor, J kg^{-1} °C^{-1}
RH	relative humidity (%)
RH_e	equilibrium relative humidity, %
RKB	Rice Knowledge Bank
t_e	equivalent drying time, min
T_o	inlet air temperature, °C
T_e	equilibrium drying air temperature, °C
T_f	final air temperature, °C
t	tonne
v	superficial air velocity, m s^{-1}
ρ_g	bulk density of grain, kg m^{-3}
ρ_a	density of air, kg m^{-3}
ΔH	change in humidity ratio, kg kg^{-1}
ΔL	difference between latent heat of vaporization of water in grain and free water, kJ kg^{-1}
Δt	time interval, min
Δx	depth of thin layer, m

Highlights

- Modeling paddy drying processes for conventional and reversible airflow FBDs
- Simulating grain moisture content and temperature profiles for different drying conditions
- Predicting timing for mixing grain and timing for reversing air affects drying performance for optimization
- Investigating relative errors between results from modeled and actual drying processes
- The error was highest at the early two-thirds stage of drying process, maximum at 19%
- the error was least at 10% at the end of drying processes.

Acknowledgments

This research was partially funded by Flagship Program 2, Upgrading Rice Value Chains, of the Consultative Group on International Agricultural Research (CGIAR) Research Program on RICE.

The authors acknowledge the valuable support of the team of Mechanization and Postharvest Cluster, Sustainable Impact Platform, the International Rice Research Institute.

The authors also acknowledge the colleagues from the Nong Lam University in Vietnam: Dr. Phan Hieu Hien, Mr. Nguyen Van Xuan, Dr. Nguyen Thanh Nghi, and Mr. Le Quang Vinh for their sharing the valuable related publications.

Disclosure statement

No potential conflict of interest was reported by the authors.

Funding

This work was supported by the RICE Flagship project 2: Upgrading rice value chains (http://ricecrp.org/wp-content/uploads/2017/01/Flagship-project-2.pdf).

ORCID

Nguyen Van Hung http://orcid.org/0000-0001-7668-6940

References

Abe, T., & Afzal, T. M. (1997). Thin-layer infrared radiation drying of rough rice. *Journal of Agricultural Engineering Research*, *67*, 289–297.

ASAE. (1997). *ASAE standards*. St. Joseph, Michigan: American Society of Agricultural Engineers.

ASAE. (1999). *Thin-Layer drying of grains and crops* (pp. 581–583). St. Joseph, Michigan: ASAE standards S448.

Brooker, D. B., Bakker-Arkema, F. W., & Hall, C. W. (1974). *Drying cereal grains*. Westport, Connecticut, USA: The AVI Publishing Co.

Chen, Y. L. (1998). A new thin-layer equation for intermittent drying of rough rice. *Journal of Agricultural Machinery*, *6*(2), 81–89.

Chen, Y. L., & Shei, H. J. (1996). Development of thin-layer equation for rough rice drying at beginning period. *Memorial College of Agriculture*, *36*(4), 321–328.

Chua, K. J., Chou, S. K., Hawlader, N. A., Mujumdar, A. S., & Ho, J. C. (2002). Modeling the moisture and temperature distribution within an agricultural product undergoing time-varying drying schemes. *Biosystems Engineering*, *81*(1), 99–111.

Dimitriadis, N. A., & Akritidis, C. B. (2004). A model to simulate chopped alfalfa drying in a fixed deep bed. *Drying Technology*, *22*(3), 479–490.

FAO (2013). Postharvest food losses estimation. Retrieved from http://www.fao.org/fileadmin/templates/ess/documents/meetings_and_workshops/GS_SAC_2013/Improving_methods_for_estimating_post_harvest_losses/Final_PHLs_Estimation_6-13-13.pdf

Felipe, C. A. A., & Barrozo, M. A. S. (2003). Drying of soybean seeds in a concurrent moving bed: Heat and mass transfer and quality analysis. *Drying Technology*, *21*(3), 439–456.

Gummert, M. (2013). Improved postharvest technologies and management for reducing postharvest losses in rice. *Acta Horticulturae*, *1011*(2013), 63–70.

Hunter, A. (1989). On the heat of sorption of Australian paddy rice. *Journal of Agricultural Engineering Research*, *44*(3), 237–239.

Islam, M., & Jindal, V. K. (1981). Simulation of paddy drying under tropical conditions. *Ama*, *12*(3), 37–41.

Jindal, V. K., & Siebenmorgen, T. J. (1994). Simulation of low-temperature paddy and rewetting in shallow beds. *Transaction of ASAE*, *37*(5), 224–228.

Kalbasi, M. (2003). Heat and moisture transfer model for onion drying. *Drying Technology*, *21*(8), 1575–1584.

Lam, T. H. (2004). *Investigation of reversible air flatbed dryer* (MSc. thesis in Agricultural Engineering). Nong Lam University, Vietnam.

Le, Q. V. (2011). *Comparative study of the performance of the reversible airflow dryer and the conventional flatbed dryer* (M. Sc. thesis in Agricultural Engineering). CLSU, Philippines.

Lopez, A., Pique, M. T., & Romero, A. (1998). Simulation on deep bed drying of hazelnuts. *Drying Technology*, *16*, 651–665.

Madhiyanon, T., Soponronnarit, S., & Tia, W. (2001). A two-region mathematical model for batch drying of grains in a two-dimensional spouted bed. *Drying Technology*, *19*(6), 1045–1064.

Martinez, R. C. (2001). *Modelling and simulation of the two-stage rice drying system in the Philippines. Forschungsbericht Pschungsbericht Agrartechnik des Arbeitskreises Forschung und Lehre der Max-Eyth-Gesellschaft Agrartechnik im VDI (VDI-MEG) 379*. Stuttgart: Universitaet Hohenheim. pp. 165.

Nguyen, T. N., Nguyen, V. X., Le, V. B., & Phan, H. H. (2009). Results of research on the 25-kg/h semi-automatic rice husk furnace. *Journal of Agricultural Science and Technology*, *2* (2009), 50–56.

Nguyen, V. H., Duong, T. H., & Gummert, M. (2016). Building a model for the paddy columnar dryer and analyzing a

reverse-airflow approach to achieve uniform grain temperature. *International Agricultural Engineering Journal*, *25* (1), 64–73.

Nguyen, V. H., Carlito, B., Quilty, J., Bojern, S., Demont, M., & Gummert, M. (2017). Processing rice straw and rice husk as co-products. In T. Sasaki (Ed.), *Achieving sustainable cultivation of rice* (Vol. 2, pp. 121–148): Burleigh Dodds Science Publishing, Series No. AS04. http://bdspublishing.com/_webedit/uploaded-files/All%20Files/Leaflets/Rice%20A4%202pp.pdf

Nguyen, V. H., Quilloy, R., & Gummert, M. (2018). Improving energy efficiency and developing an air-cooled grate for the downdraft rice husk furnace. *Renewable Energy*, *115*, 969–977.

Phan, H. H., Nguyen, H. T., Truong, V., & Nguyen, Q. L. (1995). *Grain drying in Vietnam: Problems and priorities*. Grain drying in Asia. *Proceedings of an International Conference held at the FAO Regional Office for Asia and the Pacific*. (pp. 57–67) http://ageconsearch.umn.edu/bitstream/134747/2/PR071.pdf.

Phan, H. H., Nguyen, V. X., & Nguyen, H. T. (2003, December 11–12). *Study on the reversal timing for the SRA reversible dryer*. In: *Proceeding on Agricultural Engineering and Agro-products Processing towards Mechanization and Modernization in Rural Areas* at Nong Lam University. Ho Chi Minh City.

Phan, H. H., Nguyen, V. X., Nguyen, H. T., Le, V. B., & Truong, V. (2000). *Grain dryers in Vietnam*. Vietnam ((in Vietnamese)) : Agricultural Publisher. pp. 250p.

Ricestat (2017). World rice. Retrieved from http://ricestat.irri.org/mistig/demos/php/global.php.

RKB (2017). Paddy drying. Retrieved from http://rkb.irri.org/step-by-step-production/postharvest/drying

Sitompul, J. P., Istadi, I., & Widiasa, I. N. (2001). Modeling and simulation of deep-bed grain drying. *Drying Technology*, *19*(2), 269–280.

Tado, C. J., Ona, D. P., Abon, J. E. O., Gagelonia, E., Nguyen, T. N., & Le, Q. V. (2015). Development and promotion of the reversible airflow flatbed dryer in the Philippines. *Annals of Tropical Research*, *37*(1), 97–109.

Tajaddodi, K. (2012). *Fixed Bed Drying of Rice with Air Flow Reversal for Product Quality and Drying Performance* (PhD Thesis). Malaysia: Universiti Putra Malaysia (UPM). pp. 200–205

Tang, Z., Cenkowski, S., & Muir, W. E. (2004). Modelling the superheated-steam drying of a fixed bed of brewers' spent grain. *Biosystems Engineering*, *87*(1), 67–77.

Thompson, T. L. (1972). Temporary storage of high-.moisture shelled corn using continuous aeration. *Transactions of the ASAE*, *15*(2), 333–337.

Thompson, T. L., Peart, R. M., & Foster, G. H. (1968). Mathematical modelling of corn drying – A new model. *Transactions of the ASAE*, *11*(4), 582–586.

Tran, V. T., Tran, C. T., Nguyen, T. N., & Nguyen, V. X. (2015). *Results of researching and application on automatic-fed rice husk furnace*. In: *Proceedings of 4th national science and technology seminar on engineering* (pp.739–749), Ho Chi Minh City.

Wongwises, S., & Thongprasert, M. (2000). Thin layer and deep bed drying of long grain rough rice. *Drying Technology*, *18* (7), 1583–1599.

Wratten, F. D., Poole, W. D., Chesness, J. L., Bal, S., & Ramarao, V. (1969). Physical and thermal properties of rough rice. *Transactions of the ASAE*, *12*(6), 801–803.

Xiao, H. W., & Gao, Z. J. (2008). Research progress in the effects of drying on feeding maize and processing quality. *Transactions of the Chinese Society of Agricultural Engineering*, *24*(7), 290–295.

Zare, D., & Chen, G. (2009). Evaluation of a simulation model in predicting the drying parameters for deep-bed paddy drying. *Computers and Electronics in Agriculture*, *68*(2009), 78–87.

Zare, D., Minaei, S., Zadeh, M. M., & Khoshtaghaza, M. H. (2006). Computer simulation of rough rice drying in a batch dryer. *Energy Conversion and Management*, *47*(18–19), 3241–3254.